PROCEEDINGS B

royalsocietypublishing.org/journal/rspb

Research

Cite this article: Kimmitt AA *et al*. 2023 Genetic evidence for widespread population size expansion in North American boreal birds prior to the Last Glacial Maximum. *Proc. R. Soc. B* **290**: 20221334.
https://doi.org/10.1098/rspb.2022.1334

Received: 8 July 2022
Accepted: 19 December 2022

Subject Category:
Evolution

Subject Areas:
evolution, genomics

Keywords:
demographic history, Bayesian skyline plot, migratory birds

Author for correspondence:
Benjamin M. Winger
e-mail: wingerb@umich.edu

†Present Address: Spring Island Trust, Okatie, SC 29909 USA.

Electronic supplementary material is available online at https://doi.org/10.6084/m9.figshare.c.6373159.

THE ROYAL SOCIETY PUBLISHING

Genetic evidence for widespread population size expansion in North American boreal birds prior to the Last Glacial Maximum

Abigail A. Kimmitt[1], Teresa M. Pegan[1], Andrew W. Jones[2,†], Kristen S. Wacker[1], Courtney L. Brennan[2], Jocelyn Hudon[3], Jeremy J. Kirchman[4], Kristen Ruegg[5], Brett W. Benz[1], Rachael Herman[1,6] and Benjamin M. Winger[1]

[1]Department of Ecology and Evolutionary Biology and Museum of Zoology, University of Michigan, Ann Arbor, MI 48109, USA
[2]Department of Ornithology, Cleveland Museum of Natural History, Cleveland, OH 44106, USA
[3]Royal Alberta Museum, Edmonton, Alberta Canada, T5J 0G2
[4]New York State Museum, Albany, NY 12230, USA
[5]Biology Department, Colorado State University, Fort Collins, CO 80521, USA
[6]Department of Ecology and Evolution, Stony Brook University, Stony Brook, NY 11794, USA

AAK, 0000-0003-0044-8297; BMW, 0000-0002-2095-2020

Pleistocene climate cycles are well documented to have shaped contemporary species distributions and genetic diversity. Northward range expansions in response to deglaciation following the Last Glacial Maximum (LGM; approximately 21 000 years ago) are surmised to have led to population size expansions in terrestrial taxa and changes in seasonal migratory behaviour. Recent findings, however, suggest that some northern temperate populations may have been more stable than expected through the LGM. We modelled the demographic history of 19 co-distributed boreal-breeding North American bird species from full mitochondrial gene sets and species-specific molecular rates. We used these demographic reconstructions to test how species with different migratory strategies were affected by glacial cycles. Our results suggest that effective population sizes increased in response to Pleistocene deglaciation earlier than the LGM, whereas genetic diversity was maintained throughout the LGM despite shifts in geographical range. We conclude that glacial cycles prior to the LGM have most strongly shaped contemporary genetic diversity in these species. We did not find a relationship between historic population dynamics and migratory strategy, contributing to growing evidence that major switches in migratory strategy during the LGM are unnecessary to explain contemporary migratory patterns.

1. Introduction

Glaciation cycles throughout the Quaternary have shaped current-day global biodiversity patterns, including species distributions and genetic structure [1]. Range shifts in response to changes in habitat suitability during glacial cycles have allowed species to persist in the face of climate oscillations [2,3], and such historic changes in geography are hypothesized to be associated with changes in effective population size (N_e). A widespread presumption is that Northern Hemisphere species experienced northward range shifts and concomitant population size expansions in the wake of glacial retreat following the Last Glacial Maximum (LGM; approximately 21 000 BP) [2,4–12], and studies have concluded that post-LGM expansion of bottlenecked populations explain the low levels of contemporary genetic structure and variation often observed in high latitude species (e.g. [11,13,14]). Recent studies, however, have provided genetic evidence

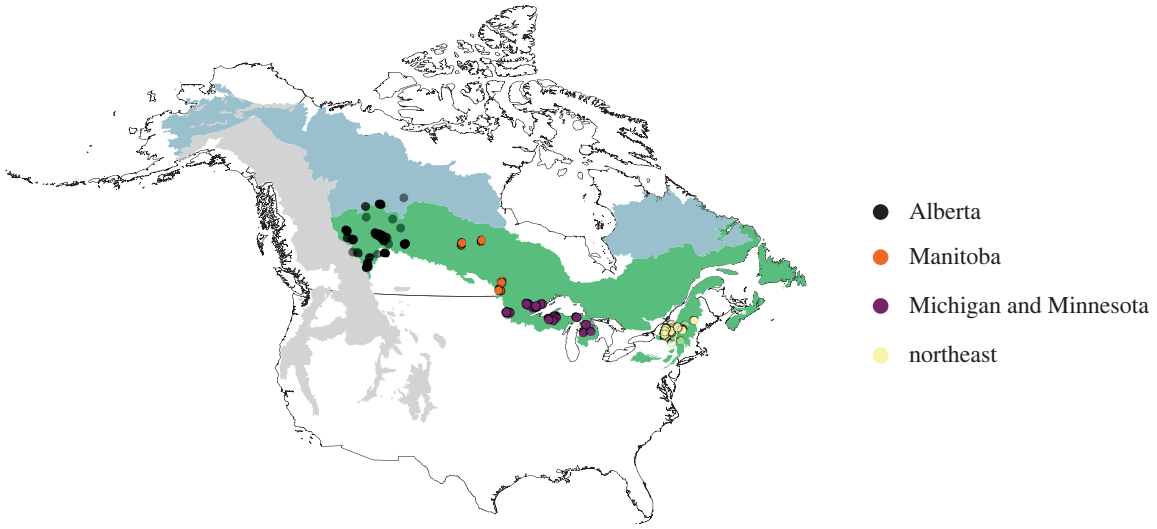

Figure 1. Map of specimen sampling locations for all 19 species. We sampled an average of 41.9 individuals (range = 24–53) per species from three to four regions of the boreal forest (colour of the points reflects the sampling location): (i) central Alberta, (ii) Manitoba, (iii) northern Michigan and Minnesota, and (iv) the northeast United States (Adirondack and Green Mountains of New York and Vermont). Each point represents an individual, such that darker shading indicates multiple individuals. The boreal forest (green), taiga (light blue) and Rocky Mountains (grey) are designated following 'level 1' ecoregions defined by Omernik & Griffith [30].

that temperate and boreal taxa may have experienced substantial population size reductions and recovery prior to the LGM [15–17]. These results raise an underexplored possibility that earlier glacial cycles have shaped contemporary population genetic patterns more than previously thought [18,19], with potential relative stability of N_e through the LGM despite obvious shifts in geographical range. The dynamics of biodiversity persistence through the LGM remains an important area of inquiry at the intersection of evolution, palaeoecology and earth science [3,5].

The relationship between glacial-interglacial range shifts and population dynamics has particular significance for migratory species breeding in the Northern Hemisphere. Like most north-temperate species, periods of glaciation must have either restricted migratory species' breeding ranges to more southerly latitudes than exist today or forced species into northern glacial refugia [7,20–22]. Because the migratory behaviour of a population is intrinsically linked to its biogeography (i.e. location of breeding and non-breeding ranges [23,24]), the impact of Pleistocene range shifts on seasonal migration has been the subject of recent debate [17,25–27]. Owing to the dearth of fossil evidence that could illuminate historical migratory patterns in birds [25,28,29], evaluating changes in migration patterns throughout time requires modelling of historical dynamics based on information from contemporary populations.

Here, we investigate how glacial cycles have shaped population dynamics of migratory species by sequencing nearly 800 mitochondrial genomes to model the demographic history of 19 avian species with broadly overlapping breeding ranges and varying migratory distances to their wintering ranges. These species breed across boreal and temperate forest of North America and winter across an array of temperate and tropical latitudes (figure 1). Previous work on a smaller number of species has shown that co-distributed boreal bird species often exhibit congruent phylogeographic patterns [27,31–33], but how these patterns relate to Pleistocene population dynamics remains poorly understood. We used low-coverage whole-genome sequencing, which enabled us to sample full mitochondrial protein-coding gene sets at high coverage from many individuals [6,34]. By sequencing many species, individuals and mitochondrial genes, we test whether members of the sympatric species assemblage that presently occupy the previously glaciated North American boreal forest exhibit evidence of population size change during the Pleistocene and whether the timing of population expansions corresponds with glacial retreat following the LGM.

A general challenge of using genetic data to infer the timing of historical events is that results can vary greatly depending on the DNA substitution rate used in analyses [35–37] and the extent to which genetic markers are evolving under the neutral coalescent. Although genome-wide multilocus data have become straightforward to gather and have several advantages over single-locus data for historical demography [38–40], gene- and taxon-specific substitution rates appropriate for historical demographic models are generally lacking [19,41–44]. By contrast, the molecular evolution of mitochondrial DNA (mtDNA) in birds has been the subject of much study [45–50], providing the opportunity to compare historical demographic scenarios under a range of previously inferred substitution rates. We modelled changes in population size over time using mass-corrected substitution rates and compare results under alternative fossil calibrations of nucleotide substitution rates [47].

We also assess how species with different migratory strategies were affected by glacial cycles. LGM range shifts have been considered so severe that they have been predicted to force the loss of migratory behaviour as species shifted towards the equator (migratory switch), such that modern long-distance migratory species shifted to breed year-round in their low-latitude, tropical wintering ranges [7,51]. For example, based on species distribution models (SDMs), Zink & Gardner [51] inferred that the putative tropical winter ranges of long-distance migrants were similar in size or even larger at the LGM, which they considered to be evidence that these species abandoned their migratory lifestyle to occupy tropical ranges year-round at the LGM. By contrast, they concluded that temperate-breeding short-distance migrants (those that currently

Table 1. Summary of the species used from the boreal system, including family and species, migratory distance (MD) and mass for species (Winger & Pegan [53]), sample size (N), average pairwise F_{ST} and Tajima's D (D). (Pairwise F_{ST} was calculated based on Weir & Cockerham [54], which can yield negative values; however, all negative F_{ST} values were rounded to zero. In *Regulus satrapa*, a species that exhibited some evidence of population structure, we conducted final analyses on a subset of geographically adjacent populations without structure. Subset sample sizes for the subset are reported in parentheses. Tajima's D and average pairwise F_{ST} are calculated from the subset of populations without structure.)

family	species	MD (km)	mass (g)	N	F_{ST}	D
Picidae	*Sphyrapicus varius*	2578	50.3	48	0.07	−2.26
Picidae	*Dryobates villosus*	0	70.4	39	0.01	−2.58
Tyrannidae	*Empidonax flaviventris*	3939	11.6	38	0.07	−2.32
Tyrannidae	*Empidonax alnorum*	6531	12.8	34	0.02	−2.27
Vireonidae	*Vireo solitarius*	2740	16.6	49	0	−2.1
Vireonidae	*Vireo olivaceus*	6739	16.7	46	0.04	−2.01
Regulidae	*Corthylio calendula*	2387	6.7	30	0	−2.47
Regulidae	*Regulus satrapa*	1492	6.2	35 (31)	0	−2.47
Turdidae	*Catharus fuscescens*	7401	31.2	39	0.06	−2.24
Turdidae	*Catharus ustulatus*	6204	30.8	51	0	−2.55
Turdidae	*Catharus guttatus*	2318	31	44	0	−2.71
Passerellidae	*Junco hyemalis*	1457	19.9	47	0.04	−2.43
Passerellidae	*Zonotrichia albicollis*	1749	25.9	53	0.01	−2.54
Passerellidae	*Melospiza lincolnii*	2909	17.4	50	0.03	−2.46
Parulidae	*Geothlypis philadelphia*	4729	12.6	36	0.09	−1.65
Parulidae	*Setophaga fusca*	5147	9.7	40	0	−2.53
Parulidae	*Setophaga palmarum*	2962	10.3	44	0.01	−2.4
Parulidae	*Setophaga coronata*	2555	12.5	49	0.02	−2.45
Parulidae	*Setophaga virens*	3861	8.8	24	0.14	−1.14

winter in temperate regions closer to their breeding grounds) were more likely to have retained sufficient—though still reduced—breeding areas in North America to persist at northern latitudes through the LGM. Other studies have similarly suggested that contemporary migratory behaviour has evolved via rapid population expansion from a subtropical ancestor since the LGM [7,14]. However, several subsequent studies have challenged these ideas [17,25–27], finding evidence that long-distance migrants could have persisted during the Late Pleistocene (126 000–11 700 BP [52]) at breeding latitudes where seasonal migration to lower non-breeding latitudes was maintained. If contemporary boreal long-distance migrants switched to become year-round tropical birds during the LGM, we predict that long-distance migrants would have larger historic N_e than short-distance migrants owing to the occupancy of putatively larger ranges at the LGM than short-distance migrants [51]. By contrast, if a species' occupancy of northern glacial refugia did not depend on its migratory behaviour, we predict no relationship between historic N_e or the timing of population expansion and migration distance.

2. Methods

(a) Study system and sampling

Our study system includes 19 co-distributed boreal forest bird species. Two species are woodpeckers (Piciformes), and the remaining are from 10 genera and six families of songbirds (Passeriformes) (table 1). These species vary in migration distance (electronic supplementary material, figure S1) but otherwise have similar life histories (e.g. mating system, age to first breeding season; [53]) and are distributed widely across forested habitats of the boreal and the temperate-boreal transition (hemiboreal) region [30,33,55].

We sequenced DNA from frozen or ethanol-preserved specimen-vouchered tissue samples deposited in our museum institutions or obtained from other museum tissue collections (mean = 41.9 samples per species, range = 24–53 samples, total = 796 samples; electronic supplementary material, table S1). All samples were collected during the breeding season. Fieldwork was approved by the University of Michigan Institutional Animal Care and Use Committee and all relevant permitting authorities (see Ethics and Acknowledgements).

Historical demographic analyses such as the Bayesian skyline plot approach we use (hereafter 'BSP') can be confounded by population structure [35,56]. Eastern continental populations of North American boreal birds exhibit limited genetic structure across much of their large ranges, whereas western montane populations often exhibit greater genetic diversity and spatial structure [27,31,32,57,58]. Therefore, to help meet assumptions of panmixia for coalescent demographic history analysis, we limited sampling to the continental boreal forest belt east of the Rocky Mountains, from central Alberta, Canada to the northeastern United States, regardless of the extent of the full species range (figure 1). We also tested for population structure within this region (see Population Structure, below). Our sampling is ideal for our goal of inferring the timing of population expansion among co-distributed populations of many species, as opposed to discovering glacial refugia or evaluating the timing of intraspecific divergences [27,59–61]. Importantly, our sampling scheme

encompasses most of the longitudinal breadth of species' ranges as well as a likely axis of southeast to northwest expansion [27], thereby making it an appropriate system to test historical demography in these taxa. For each species, we sought to sample 10–15 individuals from each of three–four regions spanning the boreal and hemiboreal forest across northern North America (figure 1; electronic supplementary material, tables S1 and S2). These regions generally correspond to (i) central Alberta, (ii) Manitoba, (iii) northern Minnesota and Michigan, and (iv) the Adirondack and Green Mountains of New York and Vermont, respectively.

(b) Mitochondrial gene set construction

Libraries were prepared using a modified Illumina Nextera library preparation protocol [62] and then sequenced on either an Illumina HiSeq platform or Illumina NovaSeq 6000 using paired-end sequencing of 150 bp reads. De novo assembly of full mitochondrial protein-coding gene sets (13 genes) was conducted using NOVOplasty v4.3.1 [63]. We removed 27 samples from the study owing to errors in library preparation or assembly failure, resulting in a total of 796 individuals with full mitochondrial gene sets (see the electronic supplementary material, Methods for additional details).

(c) Population structure

We tested for population structure across the boreal and hemiboreal belt using a tree-based generalized mixed yule coalescent (GMYC) approach [64]. GMYC [64] is an implementation of the multi-species coalescence suitable for single-locus haploid datasets which diagnoses structure in phylogenies by testing for deviations from a single panmictic population [65–67]. Additional details of the GMYC analysis are provided in the electronic supplementary material, Methods. We also calculated average pairwise fixation index (F_{ST}) between populations as an additional test of population structure. F_{ST} was calculated by binning samples into four populations (Alberta, Manitoba, Michigan + Minnesota and New York + Vermont; figure 1) and using R packages adegenet v 2.1.5 [68] and hierfstat v 0.5–10 [69] (table 1).

(d) Demographic inference

We first tested for signatures of population expansion in each species by calculating Tajima's D [70] using the R package pegas v 1.1 [71]. We then constructed BSPs for each species in BEAST2 (v 2.6.6) [72]. We conducted 'bModelTest' analyses in BEAST2 on a subsample of the data ($n = 5$ species) to select the site model and parameters for BSP analyses. Based on these results, all BSP analyses were conducted using the *TN93* model of nucleotide substitutions as the site model [73]. Proportion of invariant sites was estimated, and gamma rate heterogeneity was estimated using a gamma category count of 4.

We applied a strict clock model but with a species-specific mass-corrected substitution rate [47]. Although the mechanism is poorly understood, substitution rates are known to be negatively correlated with body mass in vertebrates [74], such that body size-corrected rates are more realistic than the '2% rule' for mtDNA [47]. We further tested the influence of alternative fossil calibrations of these size-corrected rates on the inferred timing of population expansion. We followed Nabholz *et al*. [47] to calculate substitution rate for full mitochondrial protein-coding gene sets with their equation:

$$\text{substitution rate} = \frac{10^{(\text{slope} \times \log_{10}(\text{body mass}) + \text{intercept})}}{100}.$$

We used average body mass (table 1) reported in previous work [53,75]. Slopes and intercepts for alternative fossil calibrations were provided from linear models in Nabholz *et al*.: $\log_{10}$(substitution rate)–$\log_{10}$(body mass) [47].

We estimated two substitution models based on alternative fossil calibrations performed by Nabholz *et al*. (their 'calibration 2' and 'calibration 4') for the whole concatenated mitochondrial gene set and separately for an alignment of only the third codons, resulting in a total of four analyses for each species [47]. Their fossil calibrations 1–3 were based on different fossil sets and exhibited differences in the maximum bound for the Neognathae/Paleognathae split and Psittaciformes/Passeriformes split. All three calibrations, however, yielded similar divergence dates [8,47]. 'Calibration 4', unlike the other three calibrations, included a constraint (34–28 Myr) on the Oscine/Suboscine split and produced younger divergence dates in Passeriformes and therefore faster molecular rates. Using both calibrations 2 and 4 allowed us to account for uncertainty around optimal fossil calibration of passerine molecular rates [47]. Hereafter, we refer to 'calibration 2' as the 'slow calibration' and 'calibration 4' as the 'fast calibration'.

Avian body mass is more strongly negatively correlated with third codon substitution rates than substitution rates using all codons, which could result from stronger selection on the first and second codon positions [47]. Substitution rates using all codons are more similar to the widely used '2% rule' substitution rate (0.0105 substitutions site^{-1} lineage^{-1} Myr^{-1}), whereas body mass-corrected rates may be more accurate when inferred from third codons only [47]. By repeating analyses using both codon sets, we were able to test our hypotheses under different assumptions. To compare our analyses to a more standard approach used in numerous past demographic studies in birds, we also created BSPs for each species using all codons of the cytochrome *b* (cyt*b*) gene and the '2% rule' cyt*b* molecular rate [45].

All models were run six times for 50 million steps and sampled every 5000 steps with the first 10% (5 million steps) discarded as burn-in. Log and tree files were then combined using LogCombiner. BSPs were generated in Tracer (v 1.7.2) (bins = 500). Results were only used from analyses that resulted in sufficient effective sample sizes of more than 200 [76].

To identify timing of population size expansion, we constructed generalized additive models (GAMs) with the *mgcv* package (v 1.8–38) using the estimated median N_e and a smoothing term for time [77]. We then determined changepoints in the median BSP slope by extracting the second derivatives of GAMs and identifying the minimum and maximum second derivative using the *gratia* package (v 0.6.0) [78]. Visual inspection indicated that the second derivates accurately capture changepoints for all species except for *Vireo solitarius*, for which we determined of the timing of population expansion only from visual inspection of the BSP GAMs.

We also assessed the timing and synchrony of population size expansion across our species using a hierarchal ABC coalescent approach [79] described in [80]. Using the Pipemaster package [80], we estimated four parameters of the demographic change: (i) the proportion of species exhibiting synchronous demographic change (ζ), (ii) the timing of synchronous change (T_s), (iii) the mean time of demographic changes [$E(t)$], and (iv) the dispersion index. Details on the priors and model specifications are included in the electronic supplementary material, Methods.

Finally, we tested the relationship between migration distance and both historic N_e and timing of initiation of population expansion extracted from the BSP GAM analyses. Linear models were constructed for each of the calibration–codon model sets. Migration distances for all species (table 1) were estimated in previous work as the geodesic distance between breeding and winter range centroids [53]. We confirmed whether there was phylogenetic signal in both model sets for each variable with *phytools* v 1.0–1 [81] using an ultrametric molecular phylogeny constructed in Pegan & Winger [82] from Jetz *et al*. [83]. We report results from the ordinary least-squares linear regression for historic N_e

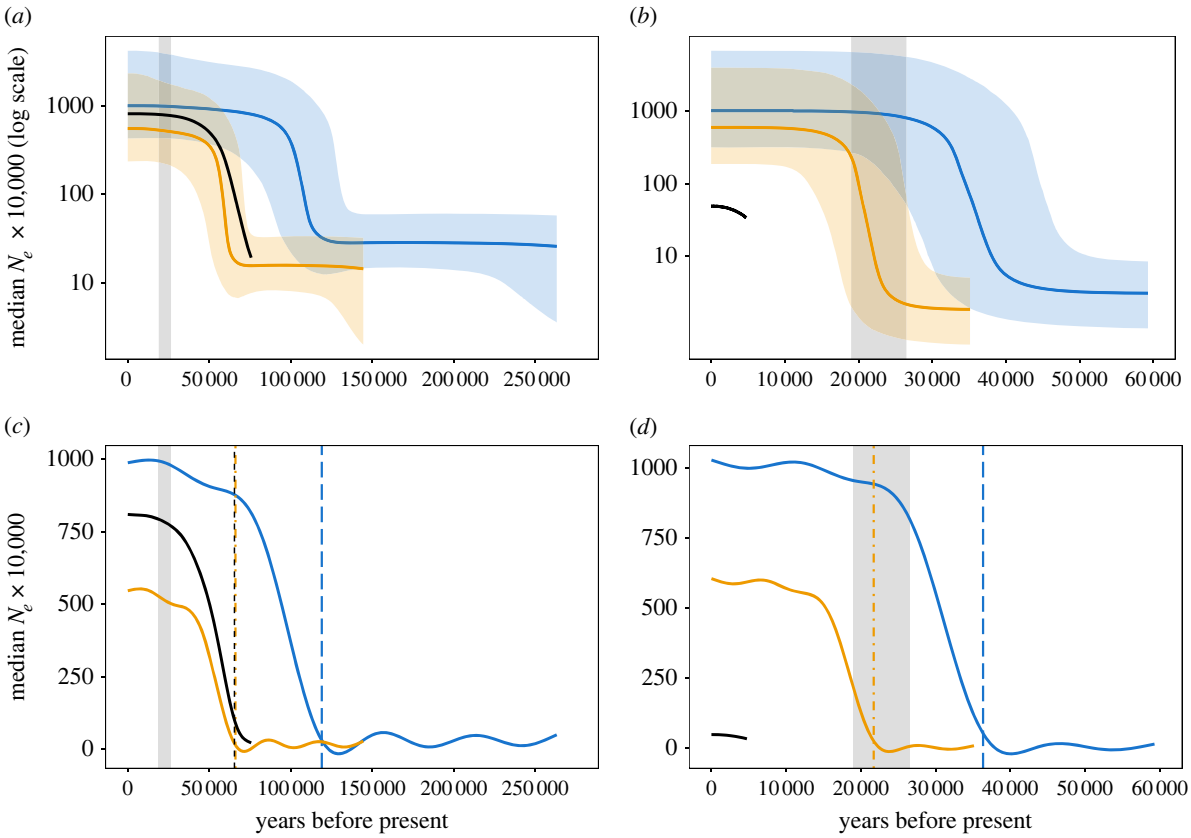

Figure 2. BSP plots for two example species, *Setophaga fusca* (*a*,*c*) and *Junco hyemalis* (*b*,*d*) to illustrate how we estimated the initiation of population size expansion. *Setophaga fusca* (*a*,*c*) is an example of a species with evidence of population size expansion prior to the LGM, whereas we found that *J. hyemalis* (*b*,*d*) probably experienced size expansion in response to deglaciation following the LGM. BSPs shown here were constructed using all codons with the slow calibration (blue) and the fast calibration (orange) substitution rates (Nabholz *et al*. [47]). The cyt*b* BSPs (black) are also shown to compare the timing of population expansions estimated with species-specific calibrations versus a standard molecular rate used on past demographic studies. The LGM (26 000–19 000 BP) is demarcated in grey. Smoothed lines and credible intervals in (*a*,*b*) are the BSP dates and population sizes output from BEAST. The *y*-axis is shown in a log scale to better visualize the credible interval around the BSP median. To quantitatively identify timing of population size expansion, we constructed GAMs using the estimated median N_e and a smoothing term for time, which are shown in (*c*,*d*). The *y*-axis in these figures is shown on a linear scale owing to negative values in the GAM fits. The dotted lines for each colour indicate approximate initiation of population expansion based on the second derivatives of the GAM slope (see Methods), which captures the relevant change in slope. Given the lack of expansion and poor resolution in the cyt*b* BSP for *J. hyemalis*, we did not identify change points or further consider estimations from this BSP for further analysis. The BSPs for all the species, including analyses using all codons and third codon only, are shown in the electronic supplementary material, figures S3–S21.

models because there was no phylogenetic signal detected in any of the models [84]. Phylogenetic signal was significant for the models evaluating initiation of population expansion ($p < 0.05$) except for the model using estimates from the cyt*b* gene ($p = 1$); therefore, we report results from phylogenetic generalized least-squares fit using maximum-likelihood and a Brownian motion correlation matrix for each calibration–codon model using *ape* v. 5.6–2 [85] and *nlme* v. 3.1–159 [86], and we report results from the ordinary least-squares linear regression for the cyt*b* model.

3. Results

Since samples were collected across the boreal belt, our *a priori* expectation was that spatial genetic structure would be low, making our study populations suitable for BSP analysis. Indeed, we found little to no geographical population structure in 18 species (electronic supplementary material, table S2 and Methods) but some evidence of structure in *Regulus satrapa* with a significantly distinct cluster of individuals in Alberta (electronic supplementary material, figure S2). Therefore, we ran the demographic analyses on a subset of individuals of *R. satrapa*, resulting in a final total of 792 full mitochondrial gene sets across all species. We also found little to no population structure in the final sample dataset pairwise F_{ST} calculations (average pairwise F_{ST}: range 0–0.14; table 1).

Consistent with expectations for population expansion, we observed significantly negative Tajima's D for 17 out of 19 of the species (table 1). Tajima's D was negative but not significant for *Geothlypis philadelphia* ($p = 0.10$) and *Setophaga virens* ($p = 0.26$).

Given that the substitution rates used (substitutions site^{-1} lineage^{-1} Myr^{-1}) do not consider generation time, the *y*-axis of the BSPs measures N_e x generation time [36]. However, since species in this study do not vary greatly in generation time (2.29 ± 0.07 years, range: 1.78–3.11 years; [87]), we did not correct for generation time and hereafter refer to the *y*-axis as estimated N_e. All species exhibited increases in N_e over time across all BSP estimations (figure 2, table 2; electronic supplementary material), except for cyt*b*-only analyses for two species (*Corthylio calendula* and *Junco hyemalis*) that exhibited population stasis, probably owing to poor resolution of the cyt*b*-only BSP (figure 2; electronic supplementary material, figures S9 and S14). Estimates for timing of population expansion for *Co. calendula* were also excluded for third codon analysis because there were no clear changepoints in the BSPs.

Table 2. Timing of population size expansion, in years before present, approximated from the second derivatives from the GAMs of the estimated median N_e from BSP analysis in BEAST and a smoothing term for time. (Cyt*b*-only analyses for two species (*Corthylio calendula* and *Junco hyemalis*) exhibited population stasis, such that we were unable to estimate change points. Estimates for timing of population expansion for *Co. calendula* were also excluded for third codon analysis because there were no clear changepoints in the BSPs.)

	timing of N_e expansion (years before present)				
species	all codons, slow calibration	all codons, fast calibration	third codon, slow calibration	third codon, fast calibration	Cyt*b*, 2% rule
Sphyrapicus varius	77 924	51 183	47 942	31 501	29 864
Dryobates villosus	118 478	79 882	49 915	33 927	34 665
Empidonax flaviventris	117 923	66 352	65 525	37 381	73 244
Empidonax alnorum	96 510	54 785	47 501	27 172	46 012
Vireo solitarius	252 107	154 511	186 893	109 897	114 637
Vireo olivaceus	196 816	114 784	119 410	70 145	107 584
Corthylio calendula	30 745	16 157	NA	NA	NA
Regulus satrapa	129 289	68 009	74 258	39 547	77 541
Catharus fuscescens	75 229	46 921	38 225	23 842	34 006
Catharus ustulatus	89 730	55 706	88 755	55 746	68 947
Catharus guttatus	46 855	29 237	28 387	17 889	23 397
Junco hyemalis	36 347	21 715	19 918	12 018	NA
Zonotrichia albicollis	83 153	50 573	54 815	34 232	53 392
Melospiza lincolnii	63 313	37 273	35 741	21 230	32 313
Geothlypis philadelphia	118 507	66 041	70 366	40 079	96 008
Setophaga fusca	118 978	66 035	68 929	38 128	65 408
Setophaga palmarum	60 538	33 488	41 692	23 748	46 711
Setophaga coronata	58 169	33 082	34 730	19 803	27 938
Setophaga virens	110 048	59 377	63 260	35 836	71 390

As expected [47], the molecular rates from the slow calibration produced older expansion dates than rates from the fast calibration (figure 3, table 2). Substitution rates that accounted for mutations at all codon positions generally yielded older expansion dates than rates based on third codon positions only (figure 3). For the slow calibration substitution rates, all 19 species were estimated to initiate population expansion prior to the LGM using all positions of the whole mitochondrial gene set (estimated range of initiation dates from BSP median values = 252 157–30 745 BP; table 2) compared to 17 out of 18 species estimated to initiate expansion prior to the LGM using third codons only (estimated range = 186 893–19 918 BP; figure 3, table 2). For the fast calibration substitution rates, 17 out of 19 species were estimated to initiate population expansion prior to the LGM for all positions of the whole mitochondrial gene set (estimated range = 154 511–16 157 BP; table 2), whereas 12 out of 18 species were estimated to initiate expansion prior to the LGM using third codons only (estimated range = 109 897–12 018 BP; figure 3, table 2). For cyt*b* analyses using the 2% rule, 15 out of 17 species were estimated to initiate expansion prior to the LGM (estimated range = 114 637–8784 BP; figure 3, table 2).

Our estimates of the timing of initiation and cessation of population size expansion based on the changes in slope of median N_e should be considered approximate, given 95% highest posterior density intervals around BSP analyses. Nevertheless, it is notable that the analyses overwhelmingly indicated an initiation of population size expansion well before the LGM for nearly all species. Our hierarchal ABC analysis also suggested that 91–92% of the species experienced synchronous population size expansion around 71 862–74 405 BP (electronic supplementary material, table S3, figure S22). We found no relationship between contemporary migratory distances and either historic N_e or timing of population expansion (table 3; electronic supplementary material, figures S24 and 25).

4. Discussion

We used advances in the estimation of mtDNA substitution rates together with full mitochondrial protein-coding gene sets to evaluate historic population dynamics from 19 co-distributed bird species that breed across the boreal forest belt in North America. Using BSP we found evidence for population size expansion in all 19 species, suggesting a demographic history of population bottlenecking sometime in the Late Pleistocene. Contrary to prior assumptions that timing of population size expansion was driven by range expansions following the LGM [2,4], we found that most species probably experienced their most dramatic population size expansion prior to the LGM. We corroborated these findings using a hierarchal ABC approach, which suggested that greater than 69% of species expanded prior to the LGM,

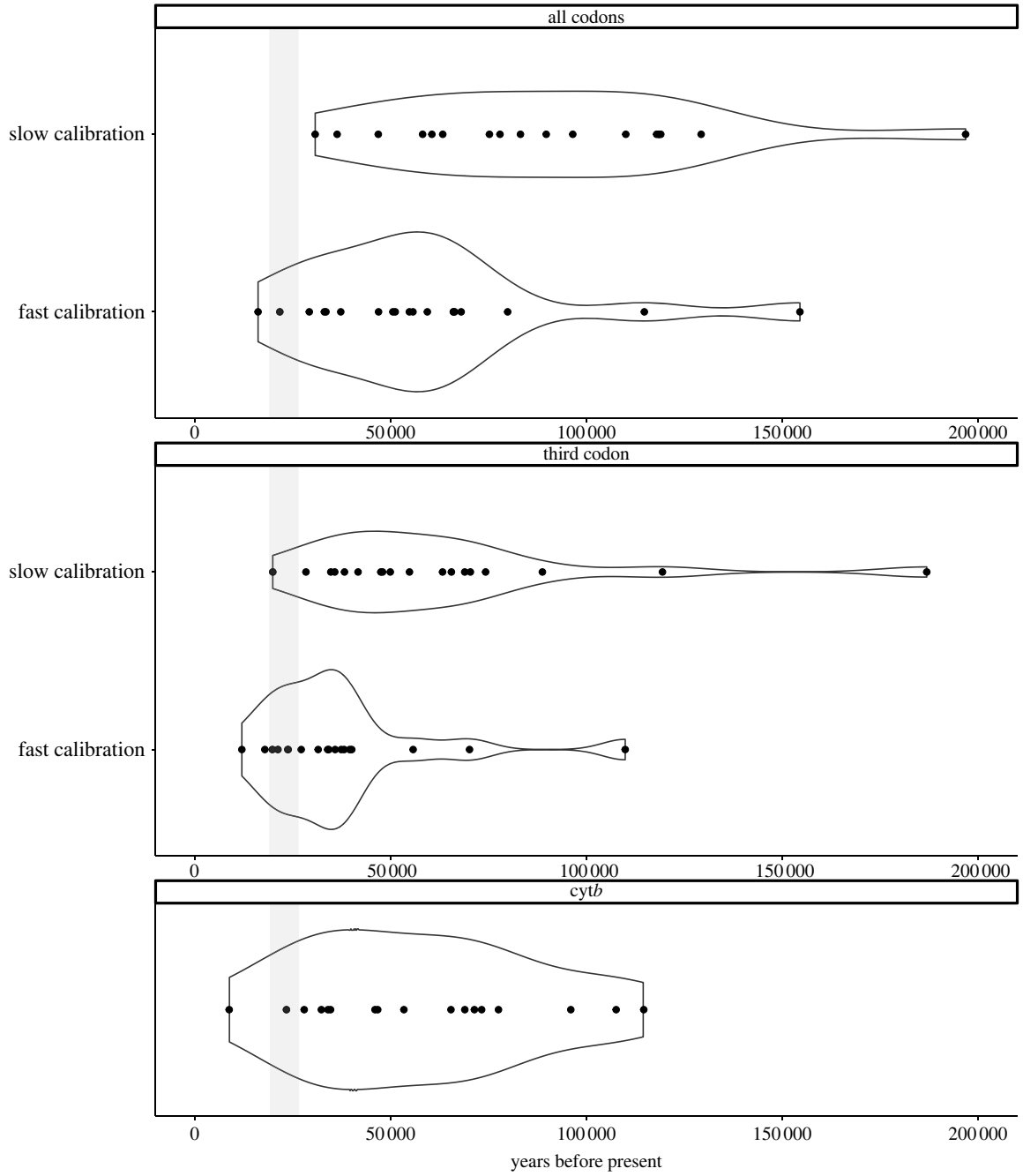

Figure 3. Comparison of timing of population size expansion (initiation of increases in N_e) across different substitution rates. Kernels show density of population expansion events whereas points are individual species population expansion events. The LGM (26 000–19 000 BP) is demarcated in grey.

with the shared expansion occurring around 64 000–75 000 BP. Interestingly, one of the few species inferred in our study to experience population expansion during or following the LGM is *J. hyemalis*, which has emerged as a classic example of rapid population expansion and differentiation following the LGM [88,89]. Our finding that the majority of co-distributed taxa probably have a different population history than the junco is robust to alternative fossil calibrations of species-specific nucleotide substitution rates and are also recovered using the 2% rule. These rates yielded a wide range of estimated dates for initiation of population size expansion [47], but expansion initiation dates were consistently prior to the LGM in the majority of species, even under demographic models that used the fastest rates. Alternative estimates of substitution rates not evaluated here include those from a study of the honeycreeper radiation [50]; these rates were faster than our slow calibration molecular rates but comparable to our fast calibration molecular rates and thus within the range of our results. Other recently calculated gene-specific molecular rates for birds [90,91] are slower than rates estimated by Nabholz *et al*. [47], such that using these rates would have estimated timing of population size expansion even earlier in history than we recover here.

For our results to be credible, two conditions must be met. First, there need to have been prior glacial cycles that could have plausibly affected the population sizes of the species in question during the Late Pleistocene. Second, population stability must have been higher than assumed through the LGM despite range displacement owing to glaciation. Recent reconstructions of glaciation throughout the Quaternary indicate that glaciation prior to the LGM peaked approximately 60 000 BP and then was followed by rapid recession of North American ice sheets during the Middle

Table 3. Results of models testing the relationship between migratory distance and (*a*) historic effective population size (N_e), and (*b*) initiation of population expansion. (N_e and initiation of population expansion estimated from each codon-calibration set of molecular rates were used in independent models. Given significant phylogenetic signal in the calibration–codon models for initiation of population expansion, we report results from phylogenetic generalized least-squares regression. For historic N_e models and the cyt*b*-only model for initiation of population expansion, we report results from the ordinary least-squares linear regression because there was no significant phylogenetic signal detected.)

historical dynamics	models	β	s.e.	p
(*a*) historic N_e	all codons (slow calibration)	67.59	130.92	0.613
	all codons (fast calibration)	44.29	81.19	0.593
	third codons (slow calibration)	−9.34	56.69	0.871
	third codons (fast calibration)	−5.07	33.71	0.882
	cyt*b*-only	10.52	115.5	0.929
(*b*) initiation of population expansion	all codons (fast calibration)	2.70	2.48	0.293
	third codons (slow calibration)	2.35	3.30	0.487
	third codons (fast calibration)	1.33	1.96	0.508
	cyt*b*-only	3.97	3.61	0.289

Wisconsin period (approx. 45 000 BP) [92,93]. Using the fast calibration, we estimate population size expansions initiated on average for all 19 species around 58 000 BP, which plausibly coincides with Middle Wisconsin deglaciation estimated from these glacial reconstructions.

Studies using genetic data to infer historic population dynamics often incorporate bioclimatic SDMs, which have been used extensively to hindcast species ranges throughout time (e.g. [10]). SDMs have provided much of the evidence for predicted range shifts and contractions throughout the glacial cycles [94]. Recent findings, however, suggest that the magnitude of range expansion estimated by SDMs may not be correlated with the magnitude of N_e changes inferred from genetic data [8]. One potential explanation for the decoupling of range size versus N_e throughout time is that SDMs assume niche conservation through time [95–97]. Predictions from SDMs do not always match fossil or pollen records, suggesting that niches can change throughout time [96,98]. Although spruce-fir (*Picea* sp.-*Abies* sp.) dominated boreal forests were probably more limited in extent during the LGM, there is evidence of widespread forested land throughout the eastern conterminous United States at the LGM [99–101]. The bird species in this study include several spruce-fir forest obligates (*sensu* [102], *Empidonax flaviventris*, *R. satrapa* and *Co. calendula*) but most of the species included here inhabit the hemiboreal region and use mixed deciduous-coniferous forest. The widespread availability of forested habitats at the LGM could have supported large N_e of contemporary hemiboreal species until northward range expansion was possible. Additionally, populations could have persisted in other proposed refugia, including current-day Newfoundland, the southern Appalachian Mountains and the Rocky Mountains [59,60,103–105]. SDM analyses exploring a slightly relaxed assumption of perfect climatic niche conservatism could help test the hypothesized maintenance of genetic diversity through the LGM, by evaluating the existence of suitable forested habitat at the LGM to support large populations.

A limitation of our study is that, although we used all 13 mitochondrial protein-coding genes, they are inherited as a single, non-recombining locus, which may not track population history closely [39,106,107] and may be subject to shared selection [108–110]. Additionally, it is possible that BSP analyses based on a single locus might only detect the most dramatic population size fluctuations and miss the signature of other, perhaps more recent, population bottlenecks and expansions. Using higher coverage whole-genome data for pairwise sequentially Markovian coalescent analysis might facilitate detection of repeated population size contractions and expansions, as seen in previous studies (e.g. [18,44,111]). However, we note that recent demographic studies of temperate birds and mammals using coalescent analysis of whole-genome data have also found similar patterns wherein the most recent substantial increase in N_e detected in some species [111] or populations [18,44] occurred prior to the LGM. Yet, owing to the widespread assumption that population size expansion should coincide with post-LGM northward range expansion, some studies have concluded that the most important expansions occurred following the LGM despite genomic evidence for pre-LGM expansion [44,112]. Our consistent results from 19 co-distributed bird species support the findings of whole-genome analyses in other taxa [44,112] and collectively point to population bottlenecking and recovery prior to the LGM as having had a potentially greater impact on shaping contemporary population genetics than the period following it for many temperate and boreal terrestrial taxa.

We also used historic N_e and timing of population expansion estimates from BSPs to explore differences in historic population dynamics considering current-day migratory behaviour. Under the 'migratory switch' hypothesis [51], species that are long-distance migrants today could have avoided population bottlenecks by switching to inhabit larger, tropical ranges year-round, whereas short-distance migratory species maintained migratory behaviour and bred in contracted ranges in the Northern Hemisphere. Instead, we found that neither historic N_e nor initiation of population expansion were correlated with current migratory distances and therefore wintering locations. Glacial cycles, including the LGM, impacted the geographical distributions of species and therefore their migratory patterns, but evidence supporting complete losses of migratory behaviour and switches to year-round residency at low latitudes remains scarce. Our finding is consistent with the growing body of literature suggesting

that long-distance migrants probably maintained seasonal migration throughout the glacial cycles [17,25–27].

In conclusion, we found strong evidence for population size expansions during the Pleistocene that predated the LGM in most of the co-occurring boreal forest bird species, contrary to hypotheses of concomitant range and population size expansions driven by deglaciation following the LGM. Instead, the timing of population expansions may coincide better with the Middle Wisconsin deglaciation (approx. 45 000 BP). Our results suggest genetic diversity was maintained through the LGM, potentially owing to sufficient forested habitat across the land in the present-day eastern United States as well as other potential refugia. The evidence from our study and other recent studies for such historic population recovery occurring earlier than previously thought provides important context for understanding modern genetic diversity and structure of temperate species, including a putatively longer period of recovered genetic diversity since the last substantial population bottleneck.

Ethics. Field sampling was approved by the University of Michigan Animal Care and Use Committee (no. PRO00010608).

Data accessibility. Genetic data generated from this study were archived on GenBank (Accession OQ034700–OQ048159). Data used for analysis are publicly available on Dryad Digital Repository (doi:10.5061/dryad.b2rbnzskk) [113] and R code is available at Zenodo (doi:10.5281/zenodo.7447931).

Additional information is also provided in the electronic supplementary material [114].

Authors' contributions. A.A.K.: conceptualization, data curation, formal analysis, investigation, methodology, validation, visualization and writing—original draft; T.M.P.: conceptualization, data curation, funding acquisition, methodology, writing—review and editing; A.W.J.: funding acquisition, writing—review and editing; K.S.W.: formal analysis, writing—review and editing; C.L.B.: writing—review and editing; J.H.: writing—review and editing; J.J.K.: writing—review and editing; K.C.R.: methodology, writing—review and editing; B.W.B.: writing—review and editing; R.H.: writing—review and editing; B.M.W.: conceptualization, data curation, formal analysis, funding acquisition, investigation, methodology, project administration, resources, supervision, validation, visualization and writing—original draft.

All authors gave final approval for publication and agreed to be held accountable for the work performed therein.

Conflict of interest declaration. We declare we have no competing interests.

Funding. This material is based upon work supported by the National Science Foundation under grant no. 2146950 to B.M.W. This research was supported by the Jean Wright Cohn Endowment Fund, Robert W. Storer Endowment Fund, Mary Rhoda Swales Museum of Zoology Research Fund and William G. Fargo Fund at the University of Michigan Museum of Zoology, and the William A. and Nancy R. Klamm Endowment funds at the Cleveland Museum of Natural History. T.M.P. was supported by the NSF Graduate Research Fellowship (DGE 1256260, Fellow ID 2018240490) and a University of Michigan Rackham Graduate Student Research Grant.

Acknowledgements. For permits to collect specimens in the field, we thank the United States Fish and Wildlife Service, the United States Forest Service, the Minnesota Department of Natural Resources, the Michigan Department of Natural Resources, the New York State Department of Environmental Conservation, Vermont Fish & Wildlife Department, Vermont Agency of Natural Resources, the Canadian Wildlife Service of Environment and Climate Change Canada, Alberta Fish and Wildlife and Manitoba Fish and Wildlife. For providing additional tissue samples, we thank the American Museum of Natural History (Brian Smith, Joel Cracraft, Paul Sweet, Peter Capainolo, Tom Trombone), Cornell University Museum of Vertebrates (Irby Lovette, Vanya Rohwer, Mary Margaret Ferraro, Charles Dardia), University of Minnesota Museum of Natural History (Keith Barker), University of California, Berkeley Museum of Vertebrate Zoology (Rauri Bowie and Carla Cicero). For assistance in the field, we thank Joe Bopp, Susanna Campbell, Shane DuBay, Gary M. Erickson, Mary Margaret Ferraro, Alyssa FitzGerald, Laura Gooch, Eric Gulson-Castillo, Joel Ralston, Corey Scobie, Vera Ting and Brian Weeks. Next-generation sequencing for this project was partially carried out in the Advanced Genomics Core at the University of Michigan. This research was also supported in part through computational resources and services provided by Advanced Research Computing (ARC), a division of Information and Technology Services (ITS) at the University of Michigan, Ann Arbor.

References

1. Svenning JC, Eiserhardt WL, Normand S, Ordonez A, Sandel B. 2015 The influence of paleoclimate on present-day patterns in biodiversity and ecosystems. *Ann. Rev. Ecol. Evol. Syst.* **46**, 551–572. (doi:10.1146/annurev-ecolsys-112414-054314)
2. Hewitt G. 2000 The genetic legacy of the Quaternary ice ages. *Nature* **405**, 907–913. (doi:10.1038/35016000)
3. Shafer AB, Cullingham CI, Cote SD, Coltman DW. 2010 Of glaciers and refugia: a decade of study sheds new light on the phylogeography of northwestern North America. *Mol. Ecol.* **19**, 4589–4621. (doi:10.1111/j.1365-294X.2010.04828.x)
4. Avise JC, Ball RM, Arnold J. 1988 Current versus historical population sizes in vertebrate species with high gene flow: a comparison based on mitochondrial DNA lineages and inbreeding theory for neutral mutations. *Mol. Biol. Evol.* **5**, 331–344.
5. Bemmels JB, Knowles LL, Dick CW. 2019 Genomic evidence of survival near ice sheet margins for some, but not all, North American trees. *Proc. Natl Acad. Sci. USA* **116**, 8431–8436. (doi:10.1073/pnas.1901656116)
6. Lou RN, Hobbs JPA, Langlois TJ, Abdo DA, Bennett S, Harvey ES. 2018 Full mitochondrial genome sequences reveal new insights about post-glacial expansion and regional phylogeographic structure in the Atlantic silverside (*Menidia menidia*). *Mar. Biol.* **165**, 1–18. (doi:10.1007/s00227-017-3259-x)
7. Milá B, Smith TB, Wayne RK. 2006 Postglacial population expansion drives the evolution of long-distance migration in a songbird. *Evolution* **60**, 2403–2409. (doi:10.1111/j.0014-3820.2006.tb01875.x)
8. Miller EF, Green RE, Balmford A, Maisano Delser P, Beyer R, Somveille M, Leonardi M, Amos W, Manica A. 2021 Bayesian skyline plots disagree with range size changes based on species distribution models for Holarctic birds. *Mol. Ecol.* **30**, 3993–4004. (doi:10.1111/mec.16032)
9. Ony M *et al.* 2021 Genetic diversity in North American *Cercis canadensis* reveals an ancient population bottleneck that originated after the Last Glacial Maximum. *Sci. Rep.* **11**, 1–16. (doi:10.1038/s41598-020-79139-8)
10. Ruegg KC, Hijmans RJ, Moritz C. 2006 Climate change and the origin of migratory pathways in the Swainson's thrush, *Catharus ustulatus*. *J. Biogeogr.* **33**, 1172–1182. (doi:10.1111/j.1365-2699.2006.01517.x)
11. Tison JL, Edmark VN, Sandoval-Castellanos E, Van Dyck H, Tammaru T, Välimäki P, Dalén L, Gotthard K. 2014 Signature of post-glacial expansion and genetic structure at the northern range limit of the speckled wood butterfly. *Biol. J. Linn. Soc.* **113**, 136–148. (doi:10.1111/bij.12327)
12. Wójcik J, Kawałko A, Marková S, Searle JB, Kotlík P. 2010 Phylogeographic signatures of northward post-glacial colonization from high-latitude refugia: a case study of bank voles using museum specimens. *J. Zool.* **281**, 249–262. (doi:10.1111/j.1469-7998.2010.00699.x)
13. Mila B, Girman DJ, Kimura M, Smith TB. 2000 Genetic evidence for the effect of a postglacial population expansion on the phylogeography of a

North American songbird. *Proc. R. Soc. Lond. B* **267**, 1033–1040. (doi:10.1098/rspb.2000.1107)

14. Malpica A, Ornelas JF. 2014 Postglacial northward expansion and genetic differentiation between migratory and sedentary populations of the broad-tailed hummingbird (*Selasphorus platycercus*). *Mol. Ecol.* **23**, 435–452. (doi:10.1111/mec.12614)
15. Burbrink FT, Chan YL, Myers EA, Ruane S, Smith BT, Hickerson MJ. 2016 Asynchronous demographic responses to Pleistocene climate change in Eastern Nearctic vertebrates. *Ecol. Lett.* **19**, 1457–1467. (doi:10.1111/ele.12695)
16. Marko PB, Hoffman JM, Emme SA, McGovern TM, Keever CC, Nicole Cox L. 2010 The 'expansion–contraction' model of Pleistocene biogeography: rocky shores suffer a sea change? *Mol. Ecol.* **19**, 146–169. (doi:10.1111/j.1365-294X.2009.04417.x)
17. Thorup K *et al.* 2021 Response of an Afro-Palearctic bird migrant to glaciation cycles. *Proc. Natl Acad. Sci. USA* **118**, e2023836118. (doi:10.1073/pnas.2023836118)
18. Taylor RS *et al.* 2021 Population dynamics of caribou shaped by glacial cycles before the Last Glacial Maximum. *Mol. Ecol.* **30**, 6121–6143. (doi:10.1111/mec.16166)
19. Nadachowska-Brzyska K, Li C, Smeds L, Zhang G, Ellegren H. 2015 Temporal dynamics of avian populations during Pleistocene revealed by whole-genome sequences. *Curr. Biol.* **25**, 1375–1380. (doi:10.1016/j.cub.2015.03.047)
20. Zink RM. 2011 The evolution of avian migration. *Biol. J. Linn. Soc.* **104**, 237–250. (doi:10.1111/j.1095-8312.2011.01752.x)
21. Mayr E, Meise W. 1930 Theoretisches zur Geschichte des Vogelzuges. *Vogelzug* **1**, 149–172.
22. Fahey AL, Ricklefs RE, Latta SC, Dewoody JA. 2012 Comparative historical demography of migratory and nonmigratory birds from the Caribbean island of Hispaniola. *Evol. Biol.* **39**, 400–414. (doi:10.1007/s11692-012-9164-9)
23. Winger BM, Auteri GG, Pegan TM, Weeks BC. 2019 A long winter for the Red Queen: rethinking the evolution of seasonal migration. *Biol. Rev.* **94**, 737–752. (doi:10.1111/brv.12476)
24. Winger BM, Barker FK, Ree RH. 2014 Temperate origins of long-distance seasonal migration in New World songbirds. *Proc. Natl Acad. Sci. USA* **111**, 12 115–12 120. (doi:10.1073/pnas.1405000111)
25. Ponti R, Arcones A, Ferrer X, Vieites DR. 2020 Lack of evidence of a Pleistocene migratory switch in current bird long-distance migrants between Eurasia and Africa. *J. Biogeogr.* **47**, 1564–1573. (doi:10.1111/jbi.13834)
26. Somveille M *et al.* 2020 Simulation-based reconstruction of global bird migration over the past 50,000 years. *Nat. Commun.* **11**, 1–9. (doi:10.1038/s41467-019-13993-7)
27. Ralston J, Fitzgerald AM, Burg TM, Starkloff NC, Warkentin IG, Kirchman JJ. 2021 Comparative phylogeographic analysis suggests a shared history among eastern North American boreal forest birds. *Ornithology* **138**, ukab018. (doi:10.1093/ornithology/ukab018)
28. Louchart A. 2008 Emergence of long distance bird migrations: a new model integrating global climate changes. *Naturwissenschaften* **95**, 1109–1119. (doi:10.1007/s00114-008-0435-3)
29. Oswald JA, Steadman DW. 2015 The changing diversity and distribution of dry forest passerine birds in northwestern Peru since the last ice age. *Auk* **132**, 836–862. (doi:10.1642/AUK-15-74.1)
30. Omernik JM, Griffith GE. 2014 Ecoregions of the conterminous United States: evolution of a hierarchical spatial framework. *Environ. Manage.* **54**, 1249–1266. (doi:10.1007/s00267-014-0364-1)
31. Adams R, Burg T. 2015 Influence of ecological and geological features on rangewide patterns of genetic structure in a widespread passerine. *Heredity* **114**, 143–154. (doi:10.1038/hdy.2014.64)
32. Burg T, Taylor SA, Lemmen KD, Gaston AJ, Friesen VL. 2014 Postglacial population genetic differentiation potentially facilitated by a flexible migratory strategy in golden-crowned kinglets (*Regulus satrapa*). *Can. J. Zool.* **92**, 163–172. (doi:10.1139/cjz-2013-0217)
33. Weir JT, Schluter D. 2004 Ice sheets promote speciation in boreal birds. *Proc. R. Soc. Lond. B* **271**, 1881–1887. (doi:10.1098/rspb.2004.2803)
34. Therkildsen NO, Palumbi SR. 2017 Practical low-coverage genomewide sequencing of hundreds of individually barcoded samples for population and evolutionary genomics in nonmodel species. *Mol. Ecol. Resour.* **17**, 194–208. (doi:10.1111/1755-0998.12593)
35. Grant WS. 2015 Problems and cautions with sequence mismatch analysis and Bayesian skyline plots to infer historical demography. *J. Hered.* **106**, 333–346. (doi:10.1093/jhered/esv020)
36. Ho SY, Shapiro B. 2011 Skyline-plot methods for estimating demographic history from nucleotide sequences. *Mol. Ecol. Resour.* **11**, 423–434. (doi:10.1111/j.1755-0998.2011.02988.x)
37. Ho SY, Lanfear R, Bromham L, Phillips MJ, Soubrier J, Rodrigo AG, Cooper A. 2011 Time-dependent rates of molecular evolution. *Mol. Ecol.* **20**, 3087–3101. (doi:10.1111/j.1365-294X.2011.05178.x)
38. Beichman AC, Huerta-Sanchez E, Lohmueller KE. 2018 Using genomic data to infer historic population dynamics of nonmodel organisms. *Annu. Rev. Ecol. Evol. Syst.* **49**, 433–456. (doi:10.1146/annurev-ecolsys-110617-062431)
39. Edwards S, Beerli P. 2000 Perspective: gene divergence, population divergence, and the variance in coalescence time in phylogeographic studies. *Evolution* **54**, 1839–1854.
40. Knowles LL. 2009 Estimating species trees: methods of phylogenetic analysis when there is incongruence across genes. *Syst. Biol.* **58**, 463–467. (doi:10.1093/sysbio/syp061)
41. Ellegren H *et al.* 2012 The genomic landscape of species divergence in *Ficedula* flycatchers. *Nature* **491**, 756–760. (doi:10.1038/nature11584)
42. Smeds L, Qvarnström A, Ellegren H. 2016 Direct estimate of the rate of germline mutation in a bird. *Genome Res.* **26**, 1211–1218. (doi:10.1101/gr.204669.116)
43. Li H, Durbin R. 2011 Inference of human population history from individual whole-genome sequences. *Nature* **475**, 493–496. (doi:10.1038/nature10231)
44. Nadachowska-Brzyska K, Burri R, Smeds L, Ellegren H. 2016 PSMC analysis of effective population sizes in molecular ecology and its application to black-and-white *Ficedula* flycatchers. *Mol. Ecol.* **25**, 1058–1072. (doi:10.1111/mec.13540)
45. Weir J, Schluter D. 2008 Calibrating the avian molecular clock. *Mol. Ecol.* **17**, 2321–2328. (doi:10.1111/j.1365-294X.2008.03742.x)
46. Zink RM, Barrowclough GF. 2008 Mitochondrial DNA under siege in avian phylogeography. *Mol. Ecol.* **17**, 2107–2121. (doi:10.1111/j.1365-294X.2008.03737.x)
47. Nabholz B, Lanfear R, Fuchs J. 2016 Body mass-corrected molecular rate for bird mitochondrial DNA. *Mol. Ecol.* **25**, 4438–4449. (doi:10.1111/mec.13780)
48. Miller EF, Manica A. 2021 mtDNAcombine: tools to combine sequences from multiple studies. *BMC Bioinf.* **22**, 115. (doi:10.1186/s12859-021-04048-0)
49. Lovette IJ. 2004 Mitochondrial dating and mixed support for the '2% rule' in birds. *The Auk* **121**, 1–6.
50. Lerner HR, Meyer M, James HF, Hofreiter M, Fleischer RC. 2011 Multilocus resolution of phylogeny and timescale in the extant adaptive radiation of Hawaiian honeycreepers. *Curr. Biol.* **21**, 1838–1844. (doi:10.1016/j.cub.2011.09.039)
51. Zink RM, Gardner AS. 2017 Glaciation as a migratory switch. *Sci. Adv.* **3**, e1603133. (doi:10.1126/sciadv.1603133)
52. Cohen KM, Finney SC, Gibbard PL, Fan JX. 2013 The ICS international chronostratigraphic chart. *Episodes J. Int. Geosci.* **36**, 199–204.
53. Winger BM, Pegan TM. 2021 Migration distance is a fundamental axis of the slow-fast continuum of life history in boreal birds. *Ornithology* **138**, 1–8. (doi:10.1093/ornithology/ukab043)
54. Weir BS, Cockram CC. 1984 Estimating *F*-statistics for the analysis of population structure. *Evolution* **38**, 1358–1370. (doi:10.2307/2408641)
55. Stralberg D, Matsuoka SM, Handel CM, Schmiegelow FKA, Hamann A, Bayne EM. 2017 Biogeography of boreal passerine range dynamics in western North America: past, present, and future. *Ecography* **40**, 1050–1066. (doi:10.1111/ecog.02393)
56. Heller R, Chikhi L, Siegismund HR. 2013 The confounding effect of population structure on Bayesian skyline plot inferences of demographic history. *PLoS ONE* **8**, e62992. (doi:10.1371/journal.pone.0062992)
57. Ruegg KC, Smith TB. 2002 Not as the crow flies: a historical explanation for circuitous migration in Swainson's thrush (*Catharus ustulatus*). *Proc. R. Soc. Lond. B* **269**, 1375–1381. (doi:10.1098/rspb.2002.2032)

58. Haché S *et al.* 2017 Phylogeography of a migratory songbird across its Canadian breeding range: implications for conservation units. *Ecol. Evol.* **7**, 6078–6088. (doi:10.1002/ece3.3170)
59. Lait L, Burg T. 2013 When east meets west: population structure of a high-latitude resident species, the boreal chickadee (*Poecile hudsonicus*). *Heredity* **111**, 321–329. (doi:10.1038/hdy.2013.54)
60. van Els P, Cicero C, Klicka J. 2012 High latitudes and high genetic diversity: phylogeography of a widespread boreal bird, the gray jay (*Perisoreus canadensis*). *Mol. Phylogenet. Evol.* **63**, 456–465. (doi:10.1016/j.ympev.2012.01.019)
61. Ralston J, Kirchman JJ. 2012 Continent-scale genetic structure in a boreal forest migrant, the blackpoll warbler (*Setophaga striata*). *Auk* **129**, 467–478. (doi:10.1525/auk.2012.11260)
62. Schweizer TM, DeSaix MG, Ruegg KC. 2021 LI-Seq: a cost-effective, low input DNA method for whole genome library preparation. *bioRxiv*. (doi:10.1101/2021.07.06.451326)
63. Dierckxsens N, Mardulyn P, Smits G. 2017 NOVOPlasty: de novo assembly of organelle genomes from whole genome data. *Nucleic Acids Res.* **45**, e18. (doi:10.1093/nar/gkw1060)
64. Pons J, Barraclough TG, Gomez-Zurita J, Cardoso A, Duran DP, Hazell S, Kamoun S, Sumlin WD, Hedin M. 2006 Sequence-based species delimitation for the DNA taxonomy of undescribed insects. *Syst. Biol.* **55**, 595–609. (doi:10.1080/10635150600852011)
65. Gehara M, Barth A, Oliveira EF, Costa MA, Haddad CB, Vences M. 2017 Model-based analyses reveal insular population diversification and cryptic frog species in the *Ischnocnema parva* complex in the Atlantic forest of Brazil. *Mol. Phylogenet. Evol.* **112**, 68–78. (doi:10.1016/j.ympev.2017.04.007)
66. Smith BT, Seeholzer GF, Harvey MG, Cuervo AM, Brumfield RT. 2017 A latitudinal phylogeographic diversity gradient in birds. *PLoS Biol.* **15**, e2001073. (doi:10.1371/journal.pbio.2001073)
67. Sukumaran J, Knowles LL. 2017 Multispecies coalescent delimits structure, not species. *Proc. Natl Acad. Sci. USA* **114**, 1607–1612. (doi:10.1073/pnas.1607921114)
68. Jombart T. 2008 adegenet: a R package for the multivariate analysis of genetic markers. *Bioinformatics* **24**, 1403–1405. (doi:10.1093/bioinformatics/btn129)
69. Goudet J. 2005 Hierfstat, a package for R to compute and test hierarchical F-statistics. *Mol. Ecol. Notes* **5**, 184–186. (doi:10.1111/j.1471-8286.2004.00828.x)
70. Tajima F. 1989 Statistical method for testing the neutral mutation hypothesis by DNA polymorphism. *Genetics* **123**, 585–595. (doi:10.1093/genetics/123.3.585)
71. Paradis E. 2010, pegas: an R package for population genetics with an integrated–modular approach. *Bioinformatics* **26**, 419–420. (doi:10.1093/bioinformatics/btp696)
72. Bouckaert R *et al.* 2019 BEAST 2.5: an advanced software platform for Bayesian evolutionary analysis. *PLoS Comput. Biol.* **15**, e1006650. (doi:10.1371/journal.pcbi.1006650)
73. Bouckaert RR, Drummond AJ. 2017 bModelTest: Bayesian phylogenetic site model averaging and model comparison. *BMC Evol. Biol.* **17**, 1–11. (doi:10.1186/s12862-017-0890-6)
74. Bromham L. 2009 Why do species vary in their rate of molecular evolution? *Biol. Lett.* **5**, 401–404. (doi:10.1098/rsbl.2009.0136)
75. Dunning JB. 2007 *CRC handbook of avian body masses*. Boca Raton, FL: CRC press.
76. Drummond AJ, Rambaut A. 2007 BEAST: Bayesian evolutionary analysis by sampling trees. *BMC Evol. Biol.* **7**, 1–8. (doi:10.1186/1471-2148-7-214)
77. Wood S. 2018. Mixed GAM computation vehicle with GCV/AIC/REML smoothness estimation and GAMMs by REML/PQL. R package version, 1-8-41. See https://cran.r-project.org/web/packages/mgcv/.
78. Simpson GL., 2018. R Package: gratia. Ggplot-based graphics and other useful functions for GAMs fitted using Mgcv, 0.1-0 (Ggplot-based graphics and utility functions for working with GAMs fitted using the mgcv package). See https://gavinsimpson.github.io/gratia/.
79. Chan YL, Schanzenbach D, Hickerson MJ. 2014 Detecting concerted demographic response across community assemblages using hierarchical approximate Bayesian computation. *Mol. Biol. Evol.* **31**, 2501–2515. (doi:10.1093/molbev/msu187)
80. Gehara M *et al.* 2017 Estimating synchronous demographic changes across populations using hABC and its application for a herpetological community from northeastern Brazil. *Mol. Ecol.* **26**, 4756–4771. (doi:10.1111/mec.14239)
81. Revell L. 2012 Bioinformatics-dendextend-an R package for visualizing, adjusting and comapring trees of hierachical clutering. *Methods Ecol. Evol* **3**, 217–223. (doi:10.1111/j.2041-210X.2011.00169.x)
82. Pegan TM, Winger BM. 2020 The influence of seasonal migration on range size in temperate North American passerines. *Ecography* **43**, 1191–1202. (doi:10.1111/ecog.05070)
83. Jetz W, Thomas GH, Joy JB, Hartmann K, Mooers AO. 2012 The global diversity of birds in space and time. *Nature* **491**, 444–448. (doi:10.1038/nature11631)
84. Revell LJ. 2010 Phylogenetic signal and linear regression on species data. *Methods Ecol. Evol.* **1**, 319–329. (doi:10.1111/j.2041-210X.2010.00044.x)
85. Paradis E. 2012 *Analysis of phylogenetics and evolution with R*, vol. **2**. Berlin, Germany: Springer.
86. Pinheiro J, Bates D, DebRoy S, Sarkar D, Team RC. 2007 Linear and nonlinear mixed effects models. R package version 3.1–89. See https://cran.r-project.org/web/packages/nlme.
87. Bird JP *et al.* 2020 Generation lengths of the world's birds and their implications for extinction risk. *Conserv. Biol.* **34**, 1252–1261. (doi:10.1111/cobi.13486)
88. Milá B, McCormack JE, Castañeda G, Wayne RK, Smith TB. 2007 Recent postglacial range expansion drives the rapid diversification of a songbird lineage in the genus Junco. *Proc. R. Soc. B* **274**, 2653–2660. (doi:10.1098/rspb.2007.0852)
89. Friis G, Aleixandre P, Rodríguez-Estrella R, Navarro-Sigüenza AG, Milá B. 2016 Rapid postglacial diversification and long-term stasis within the songbird genus *Junco*: phylogeographic and phylogenomic evidence. *Mol. Ecol.* **25**, 6175–6195. (doi:10.1111/mec.13911)
90. Arcones A, Ponti R, Vieites DR. 2021 Mitochondrial substitution rates estimation for divergence time analyses in modern birds based on full mitochondrial genomes. *Ibis* **163**, 1463–1471. (doi:10.1111/ibi.12965)
91. Pacheco MA, Battistuzzi FU, Lentino M, Aguilar RF, Kumar S, Escalante AA. 2011 Evolution of modern birds revealed by mitogenomics: timing the radiation and origin of major orders. *Mol. Biol. Evol.* **28**, 1927–1942. (doi:10.1093/molbev/msr014)
92. Batchelor CL, Margold M, Krapp M, Murton DK, Dalton AS, Gibbard PL, Stokes CR, Murton JB, Manica A. 2019 The configuration of Northern Hemisphere ice sheets through the Quaternary. *Nat. Commun.* **10**, 1–10. (doi:10.1038/s41467-019-11601-2)
93. Dalton AS, Stokes CR, Batchelor CL. 2022 Evolution of the Laurentide and Innuitian ice sheets prior to the Last Glacial Maximum (115 ka to 25 ka). *Earth Sci. Rev.* **224**, 103875. (doi:10.1016/j.earscirev.2021.103875)
94. Elith J, Leathwick JR. 2009 Species distribution models: ecological explanation and prediction across space and time. *Ann. Rev. Ecol. Evol. Syst.* **40**, 677–697. (doi:10.1146/annurev.ecolsys.110308.120159)
95. Peterson AT. 2011 Ecological niche conservatism: a time-structured review of evidence. *J. Biogeogr.* **38**, 817–827. (doi:10.1111/j.1365-2699.2010.02456.x)
96. Veloz SD, Williams JW, Blois JL, He F, Otto-Bliesner B, Liu Z. 2012 No-analog climates and shifting realized niches during the late quaternary: implications for 21st-century predictions by species distribution models. *Glob. Change Biol.* **18**, 1698–1713. (doi:10.1111/j.1365-2486.2011.02635.x)
97. FitzGerald AM, Starkloff NC, Kirchman JJ. 2018 Testing the predictive capabilities of ecological niche models: a case study examining red-bellied woodpeckers. *Ecosphere* **9**, e02496. (doi:10.1002/ecs2.2496)
98. McGuire JL, Davis EB. 2013 Using the palaeontological record of *Microtus* to test species distribution models and reveal responses to climate change. *J. Biogeogr.* **40**, 1490–1500. (doi:10.1111/jbi.12106)
99. Allen JR, Forrest M, Hickler T, Singarayer JS, Valdes PJ, Huntley B. 2020 Global vegetation patterns of the past 140,000 years. *J. Biogeogr.* **47**, 2073–2090. (doi:10.1111/jbi.13930)
100. Bemmels JB, Dick CW. 2018 Genomic evidence of a widespread southern distribution during the Last Glacial Maximum for two eastern North American

hickory species. *J. Biogeogr.* **45**, 1739–1750. (doi:10.1111/jbi.13358)

101. Beyer RM, Krapp M, Manica A. 2020 High-resolution terrestrial climate, bioclimate and vegetation for the last 120,000 years. *Sci. Data* **7**, 1–9. (doi:10.1038/s41597-020-0552-1)
102. Ralston J, King DI, Deluca WV, Niemi GJ, Glennon MJ, Scarl JC, Lambert JD. 2015 Analysis of combined data sets yields trend estimates for vulnerable spruce-fir birds in northern United States. *Biol. Conserv.* **187**, 270–278. (doi:10.1016/j.biocon.2015.04.029)
103. Dohms KM, Graham BA, Burg TM. 2017 Multilocus genetic analyses and spatial modeling reveal complex population structure and history in a widespread resident North American passerine (*Perisoreus canadensis*). *Ecol. Evol.* **7**, 9869–9889. (doi:10.1002/ece3.3478)
104. FitzGerald AM, Weir J, Ralston J, Warkentin IG, Whitaker DM, Kirchman JJ. 2020 Genetic structure and biogeographic history of the Bicknell's thrush/gray-cheeked thrush species complex. *The Auk* **137**, ukz066. (doi:10.1093/auk/ukz066)
105. Soltis DE, Morris AB, McLachlan JS, Manos PS, Soltis PS. 2006 Comparative phylogeography of unglaciated eastern North America. *Mol. Ecol.* **15**, 4261–4293. (doi:10.1111/j.1365-294X.2006.03061.x)
106. Edwards S, Bensch S. 2009 Looking forwards or looking backwards in avian phylogeography? A comment on Zink and Barrowclough 2008. *Mol. Ecol.* **18**, 2930–2933. Discussion 2934–2936. Citeseer. (doi:10.1111/j.1365-294X.2009.04270.x)
107. Toews DP, Brelsford A. 2012 The biogeography of mitochondrial and nuclear discordance in animals. *Mol. Ecol.* **21**, 3907–3930. (doi:10.1111/j.1365-294X.2012.05664.x)
108. Jensen JD, Kim Y, Dumont VB, Aquadro CF, Bustamante CD. 2005 Distinguishing between selective sweeps and demography using DNA polymorphism data. *Genetics* **170**, 1401–1410. (doi:10.1534/genetics.104.038224)
109. Johri P, Charlesworth B, Jensen JD. 2020 Toward an evolutionarily appropriate null model: jointly inferring demography and purifying selection. *Genetics* **215**, 173–192. (doi:10.1534/genetics.119.303002)
110. Stajich JE, Hahn MW. 2005 Disentangling the effects of demography and selection in human history. *Mol. Biol. Evol.* **22**, 63–73. (doi:10.1093/molbev/msh252)
111. Kozma R, Melsted P, Magnússon KP, Höglund J. 2016 Looking into the past–the reaction of three grouse species to climate change over the last million years using whole genome sequences. *Mol. Ecol.* **25**, 570–580. (doi:10.1111/mec.13496)
112. Smith CC, Flaxman SM, Scordato ESC, Kane NC, Hund AK, Sheta BM, Safran RJ. 2018 Demographic inference in barn swallows using whole-genome data shows signal for bottleneck and subspecies differentiation during the Holocene. *Mol. Ecol.* **27**, 4200–4212. (doi:10.1111/mec.14854)
113. Kimmitt AA *et al*. 2023 Data from: Genetic evidence for widespread population size expansion in North American boreal birds prior to the Last Glacial Maximum. Dryad Digital Repository. (doi:10.5061/dryad.b2rbnzskk)
114. Kimmitt AA *et al*. 2023 Genetic evidence for widespread population size expansion in North American boreal birds prior to the Last Glacial Maximum. Figshare. (doi:10.6084/m9.figshare.c.6373159)